LABORATORI NAZIONALI DI FRASCATI
SIS-Pubblicazioni

LNF-02/010 (IR)
10 Giugno 2002
CERN-Nufact-Note-108

BEAM DYNAMICS STUDY OF A MUON IONIZATION COOLING EXPERIMENT

M. Aleksa[1], J. F. Amand[1], R. Garoby[1], F. Gerigk[1], K.Hanke[1],
E. B. Holzer[1], E. S. Kim[2], A. Lombardi[1], M. Migliorati[3,4],
S. Russenschuck[1], F. Tazzioli[3], C. Vaccarezza[3]
[1)] *CERN, Geneva, Switzerland*
[2)] *Pohang Accelerator Lab, POSTECH, Pohang, Korea*
[3)] *INFN - LNF, Frascati, Italy*
[4)] *Univ. La Sapienza, Dip. Energetica, Rome, Italy*

Abstract

We present a summary of simulation results for a muon cooling experiment. Two possible scenarios have been studied: The first is a subsection of the 88 MHz cooling channel in the CERN reference scheme for a neutrino factory. The second system studied is based on 200 MHz cavities as proposed in the US study II design. The studies comprise a scan of input beam parameters, various optics with and without alternating solenoid polarity as well as a cross-check with an independent simulation code.

PACS:29.17;29.27;41.75.i;41.85.Ja

1 Introduction

The CERN layout for a neutrino factory features a cooling channel based on 44 and 88 MHz cavities with integrated super conducting solenoids [1].

In order to prove the feasibility of such a cooling channel, a cooling experiment is proposed which is a small subset of the 88 MHz part of the final channel. The first system studied consists of a total of 8 cavities at 88 MHz providing an average effective gradient of 4 MV/m. For an input kinetic energy of 200 MeV, the energy lost in a length of 94 cm of liquid hydrogen (LH_2) absorber can be replaced by these cavities and the beam energy at the end of the cooling cell is the same as at the entry. The layout of the channel is such that there is an absorber of 47 cm length at the entry of the cooling section, followed by a string of 8 cavities with integrated solenoids (total length 7.2 m) and a second absorber of 47 cm length at the exit of the cooling section. The solenoid lattice is continued upstream and downstream of the cooling cell where the input and output diagnostics are installed.

The second system studied consists of only 4 cavities of the same type (length of the accelerating section 3.6 m). This set-up allows only for a total of 47 cm liquid hydrogen, again split up into a 23.5 cm entry absorber and a 23.5 cm exit absorber. The cooling efficiency then drops down in proportion. Also this cooling cell is matched upstream and downstream to diagnostic solenoids. Figure 1 shows schematically both systems studied.

As an alternative to a cooling experiment based on 88 MHz cavities, we have studied a system at 200 MHz as proposed in the US study II design for a neutrino factory [2]. A comparison of the two systems from a beam dynamics point of view shows comparable

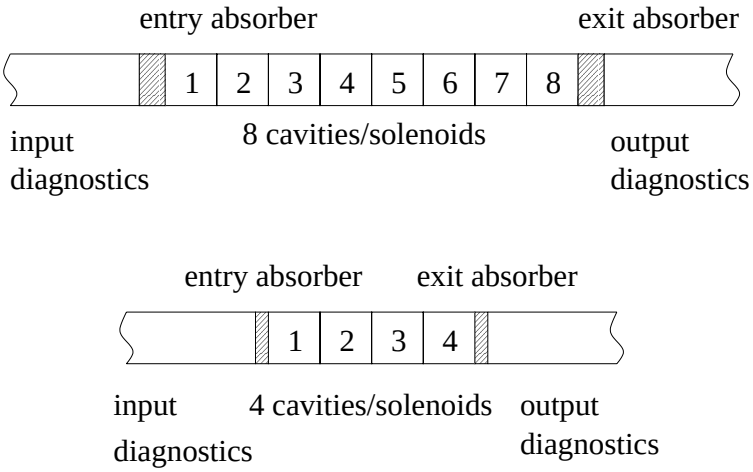

Figure 1: Set-up with 8 cavities (upper sketch) and 4 cavities (lower sketch).

cooling efficiency, while the beam optics is very different.

2 88 MHz Option

2.1 88 MHz Cavities for the Cooling Lattice

The large phase space of the muon beam requires low frequencies (88 MHz), large bore radii (0.15 m) and a high magnetic field produced by super conducting solenoids. The present approach [3] to match these demands is to incorporate the solenoids into the cavity design in order to avoid the huge dimensions of solenoids surrounding the cooling channel. Using an asymmetric cavity design (Fig. 2) enables the construction of units which consist of solenoid plus cavity and which can then be assembled to a continuous lattice.

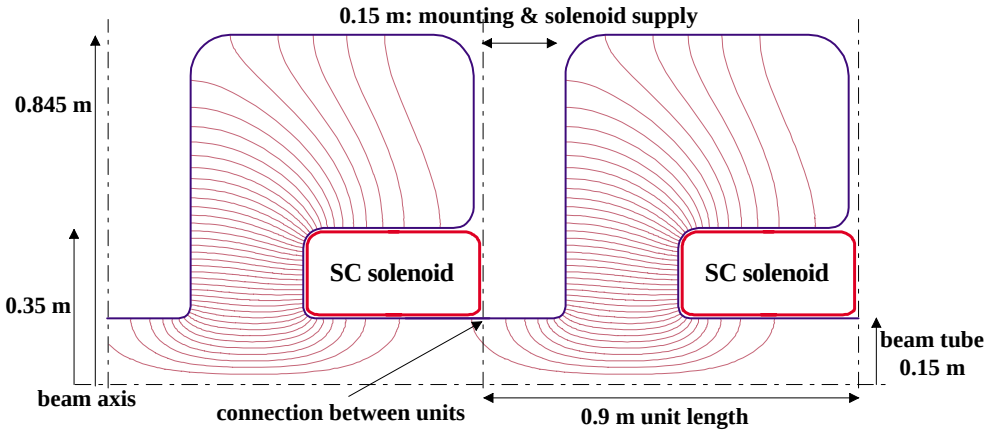

Figure 2: Scheme of assembling 88 MHz cavities with solenoids.

A higher mechanical filling factor of solenoid over unit length can be obtained by increasing the length of the solenoids by a few centimetres for the price of higher RF power consumption and bigger amplifiers delivering higher peak power (details in [3]).

Table 1: Parameters for the 88 MHz cavities (calculated by SUPERFISH)

f_{rep} [Hz]	E_0T [MV/m]	Q	R/Q [Ω]	t_{pulse} [ms]	$P_{amp.}$ [MW]	P_{mean} [kW/m]	Kilp.	$R_{cav.}$ [m]	$l_{sol.}$ [m]
50	4	44000	144	0.48	2.04	54	2.3	0.845	0.4

2.2 Solenoid Design

In the present design, super conducting solenoids are integrated into the 88 MHz cavities. They have been designed [4] using ROXIE8.1. The solenoid design takes into account engineering constraints, such as space required for the cryogenic system and forces between solenoids. Both the case with all solenoids of the same polarity and the case of opposite polarity ('field flip') have been simulated and the corresponding field maps generated. Figure 3 shows the configuration for same polarity. The field strength on axis is limited by the current density and the field strength in the coil. At 4.5 K, $NbTi$ quenches at about 9 T for the given current density. If one wants to stay below 60% on the load line, a field in the coil of 5.2 T resulting in 4.5 T on axis is the limit. Gaining field strength is possible by increasing the percentage on the load line, i.e. having a smaller quench margin. It is

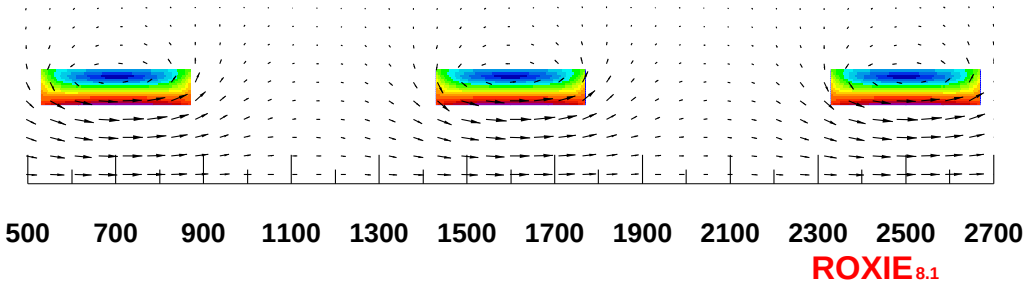

Figure 3: Solenoid design for the case of same polarity.

important to maintain a sufficient thermal margin in view of the beam energy deposited in the super conductors. Here further simulations have to be done. In case the losses can be kept small by appropriate shielding a maximum of 80% on the load line could be envisaged. In any case an appropriate quench protection has to be designed. One should also investigate working at lower temperature or using other super conductors, e.g. Nb_3Sn, in order to achieve a high field strength of about 6 T which would allow to reduce the bore of the cavities. Figure 4 shows the B_z and B_r versus z for the maximum field achievable with $NbTi$ at 4.5 K and staying below 60% on the load line. For the assumed currents (1920 kA $\times$ turns) the force between the first and second solenoid are 78 kN. Inside the cooling channel (all solenoids apart from the first and the last one) the force cancels.

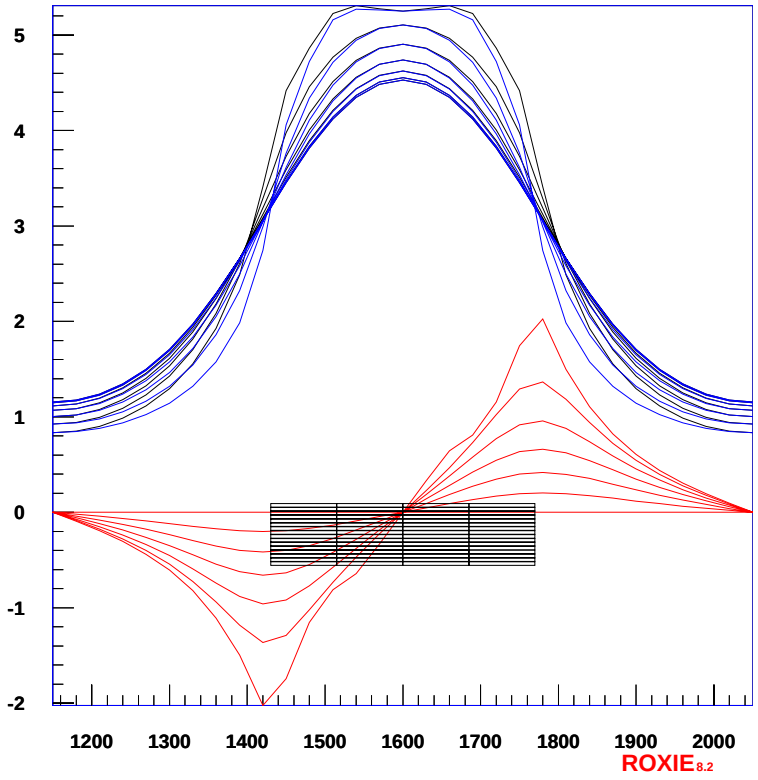

Figure 4: B_z (upper plot) in [T] and B_r (lower plot) in [T] versus z [mm] at different radii (r = 0 mm, 30 mm, ..., 180 mm) for the maximum achievable field strength of a $NbTi$ solenoid at 4.5 K and staying below 60% on the load line.

2.3 Beam Dynamics of a Channel with 8 Cavities

2.3.1 Reference Optics

A beam dynamics study of the proposed cooling channel has been performed, based on the engineering design of cavities and solenoids. The solenoid field maps have been included in the tracking code PATH. The input beam parameters have been chosen similar to those in the 88 MHz section of the CERN reference cooling channel: β= 1 m, α=0, E_{kin}=200 MeV, ΔE= $\pm$ 30 MeV. For this example case, the solenoids in the cooling cell have settings around 3 T and the cavity synchronous phase is set on crest. For this optics and appropriate input beam emittance the transmission is 100% and the transverse emittance at the exit of the cooling channel is reduced by about 3.7%. Figure 5 shows the transverse emittance versus z computed for 50000 muons.

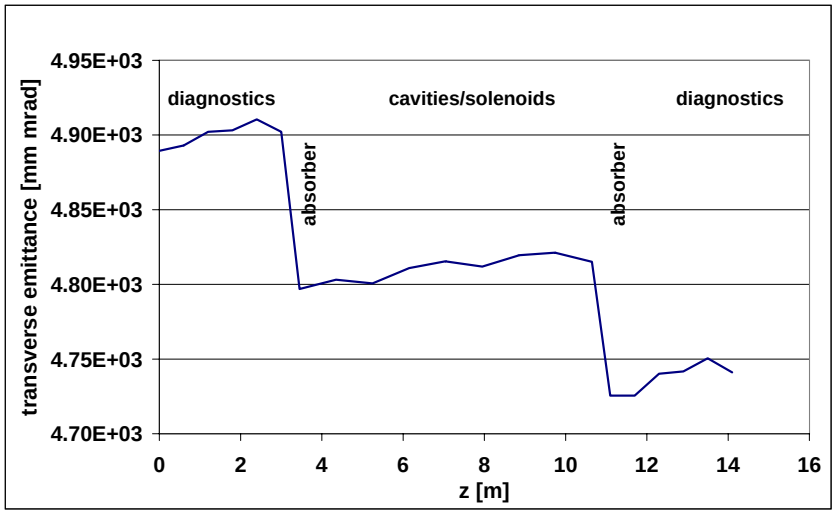

Figure 5: Transverse emittance (r.m.s., normalized) computed with PATH along the channel of 8 cavities.

2.3.2 Scan of Input Emittance

In order to determine the response of the system to various input beam parameters, parameter scans were carried out [5]. The input emittance was varied and the emittance at the exit of the channel computed. Figure 6 shows the output emittance for various values of the input emittance. For an input emittance of about 3500 π mm mrad (r.m.s., normalized), the equilibrium emittance is reached. For values below this threshold, the channel starts heating. For values between 3500 and 6000 π mm mrad, the transmission is 100% and the channel is cooling. For larger values of the input emittance, the acceptance of the channel is reached and the transmission starts to drop down. Figure 7 shows the transmission through the channel for the corresponding range of input r.m.s. emittance.

Another way to analyse the results is to count the number of muons that are found inside a given acceptance. In our case, we have chosen the acceptance of the recirculator in the CERN reference scheme, i.e. 15000 π mm mrad (normalized) in both transverse and 0.1 eVs in the longitudinal plane. Within this volume, for the example case discussed in Section 2.3.1 the number of muons is increased by 9.1 %.

The cooling efficiency, defined as the increase of the number of particles inside the given acceptance, is shown in Fig. 8 for a range of input r.m.s. emittance. Depending on the input beam emittance, the cooling efficiency goes up to 15%. Note, that positive cooling efficiency is still found for emittances larger than the acceptance of the channel, i.e. for values for which the transmission is no longer 100% (compare Fig. 7).

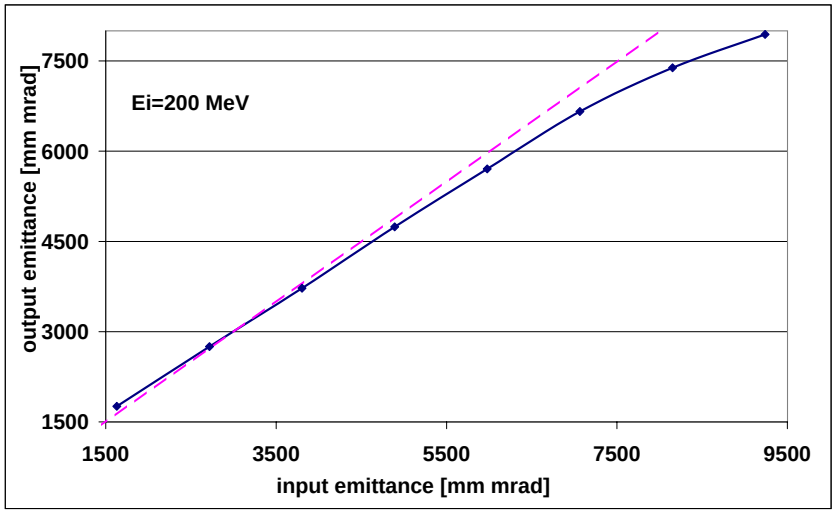

Figure 6: Output emittance versus input emittance (r.m.s., normalized) for a channel of 8 cavities and an input beam energy of 200 MeV. The dashed line means $\varepsilon_{out} = \varepsilon_{in}$. It can be seen that the channel is cooling for a wide range of input emittances. At about 6000 mm mrad, the acceptance of the channel is reached. At about 3500 mm mrad, the equilibrium emittance is reached. The solenoid and cavity settings are kept constant during the scan.

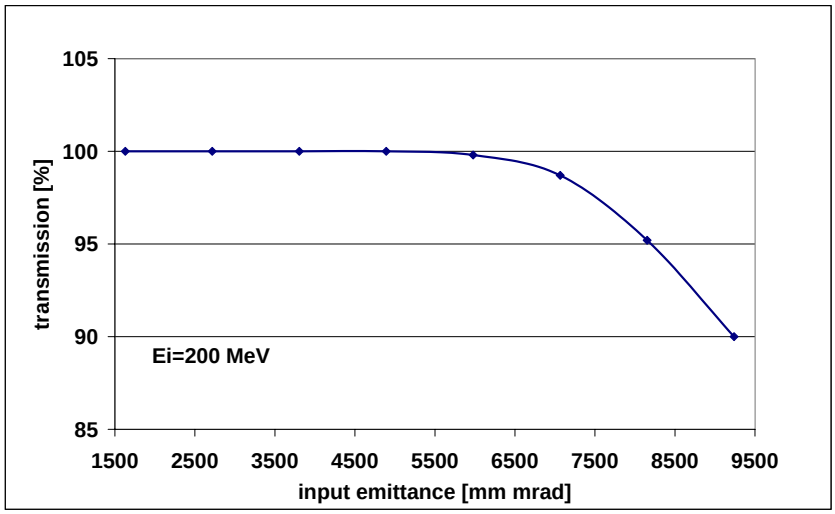

Figure 7: Transmission versus input emittance (r.m.s., normalized) for a channel of 8 cavities and an input beam energy of 200 MeV. The solenoid field in this simulation is 3 T. The acceptance is reached at about 6000 mm mrad.

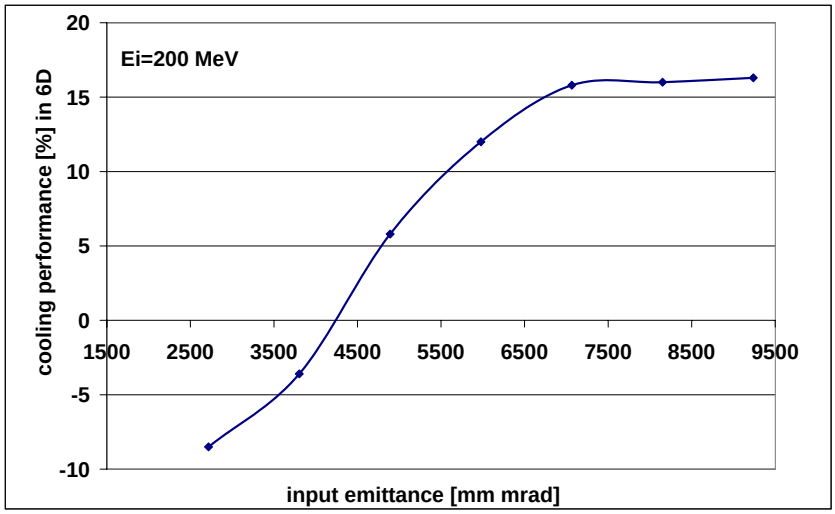

Figure 8: Cooling efficiency versus input emittance (r.m.s., normalized) for a channel of 8 cavities and an input beam energy of 200 MeV. The cooling efficiency goes up to 15% and stays at this value even beyond the acceptance of the channel. Note, that in this definition heating sets on at $\varepsilon_{in} \approx 4000$ mm mrad while Fig. 6 shows an equilibrium emittance of about 3500 mm mrad. This is due to the effect that for a very small beam size the cut is close to the beam size which influences the result. Applying a smaller cut results in a positive cooling efficiency.

2.3.3 Influence of Beam Energy

We have run the setup with 8 cavities for various input beam energies: 230 MeV, 200 MeV, 170 MeV and 140 MeV. Detailed results are reported in [5]. Figure 9 shows the cooling efficiency for the four different input beams. To summarize the parameter scan for the system with 8 cavities, we consider an input emittance of 5500 mm mrad (r.m.s., normalized), for which the transmission is 100%. The cooling efficiency for this input emittance and the various input beam energies is summarized in Tab. 2. The dependence of transmission and equilibrium emittance on the beam energy is negligible. The magnetic field in the cooling cell has a value of 2.7 T.

2.3.4 Simulations with alternating Solenoid Polarity

Running the cooling experiment in a configuration with alternating solenoid polarity (*'field flip'*) is not advantageous in terms of cooling efficiency. However, it is of importance for the final cooling channel and hence one may want to set up also the experimental channel in this configuration. The channel with 8 cavities and the example optics

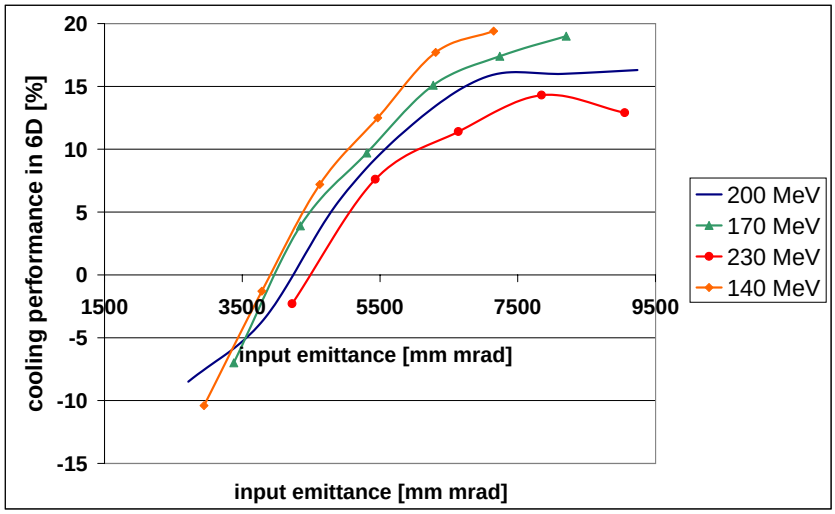

Figure 9: Cooling efficiency versus input beam emittance (r.m.s., normalized) for a system of 8 cavities and various input beam energies.

E_{in} [MeV]	cooling efficiency [%]	solenoid field [T]
230	7.5	2.7
200	10.0	2.7
170	11.5	2.7
140	12.5	2.7

Table 2: Comparison of cooling efficiency for ε_{in}=5500 mm mrad (r.m.s., normalized) and various input beam energies. The results illustrate that the 88 MHz cooling channel is broadband.

discussed in Section 2.3.1 was therefore simulated with alternating solenoid field in the cooling section. The emittance reduction is the same as in the case where all solenoids have the same polarity (Fig. 5). Figure 10 shows the transverse emittance along the channel.

2.3.5 Absorber Walls

We have re-run the configuration with 8 cavities and the reference optics and added absorber walls of 150 μm thickness. The cooling performance is affected only slightly. Figure 11 shows the transverse emittance along the channel taking into account the absorber walls.

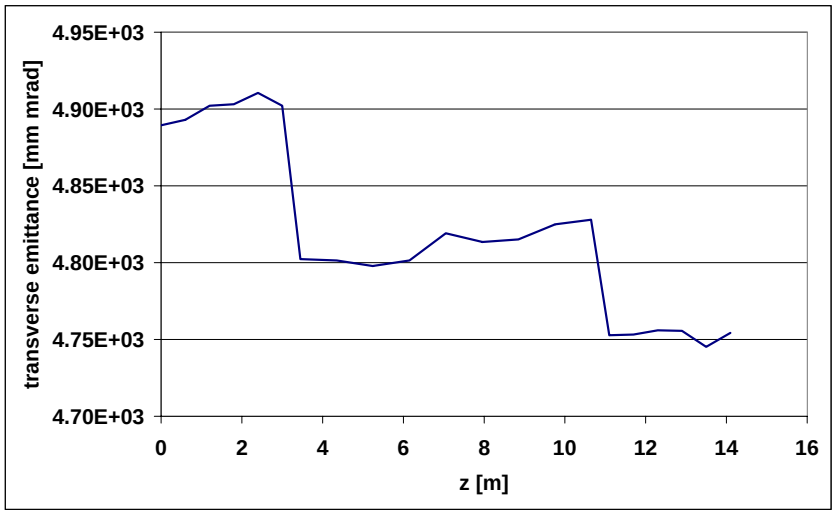

Figure 10: Transverse emittance (r.m.s., normalized) along the channel for a channel of 8 cavities and an input beam energy of 200 MeV. The polarity of the solenoids in the cooling section is alternating (*'field flip'*). The cooling performance is the same as in the case of same polarity (Fig. 5). Simulation with PATH and 50000 muons.

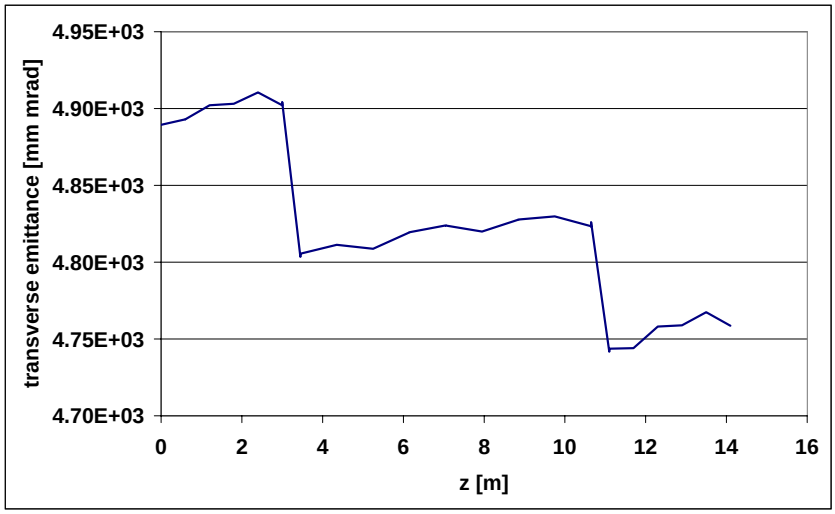

Figure 11: Transverse emittance (r.m.s., normalized) along the channel with 8 cavities at 200 MeV taking into account the absorber walls. Simulation with PATH and 50000 muons.

2.4 Electric Field Map

While in the simulations reported in the previous sections the cavities were represented by a stepwise energy increase, we have for the reference case (8 cavities, input beam and optics as in 2.3.1) performed a simulation which includes both the magnetic field map and the electric field map. These have been obtained from a SUPERFISH simulation of the cavities described in Section 2.1. The emittance evolution along the channel is shown in Fig. 12. The result is consistent with the one shown in Fig. 5.

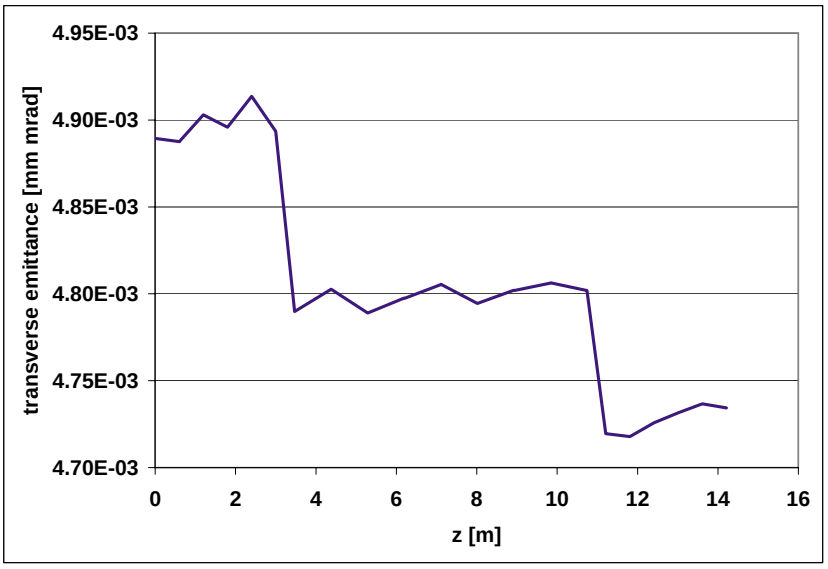

Figure 12: Transverse emittance along the channel with 8 cavities at 200 MeV taking into account both the magnetic and electric field map.

2.5 Beam Dynamics of a Channel with 4 Cavities

2.5.1 Reference Optics

Using the same optics and input beam parameters, but only 4 cavities and half the absorber length, the cooling performance of the channel drops down roughly in proportion. Figure 13 shows the transverse emittance versus z for this set-up. The reduction of the transverse emittance is in this case 2% and the number of muons inside the acceptance is increased by 3.5%.

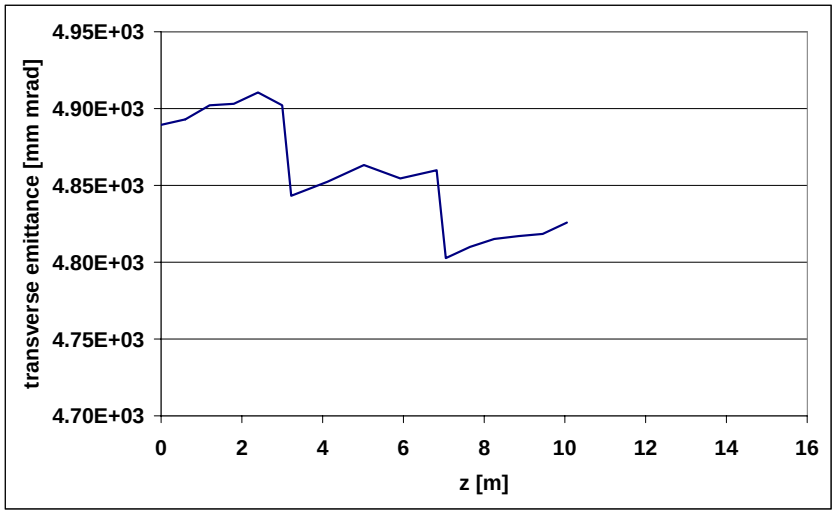

Figure 13: Transverse emittance (r.m.s., normalized) as computed by PATH along the channel for the set-up with 4 cavities. The emittance evolution along the channel is similar to the case of 8 cavities (see Fig. 5), but the length and the cooling performance drops down in proportion. PATH simulation with 50000 muons.

2.5.2 Scan of Input Emittance

Figures 14-16 show output versus input emittance, transmission and cooling efficiency for a range of input emittances and an input beam energy of 200 MeV. The acceptance of the channel is the same as for the case with 8 cavities. The cooling efficiency drops with respect to the case of 8 cavities. The maximum value is about 10%.

2.5.3 Influence of Beam Energy

As the cooling efficiency is worse than in the case of 8 cavities and it will become even worse at higher input energy than 200 MeV, we have studied a case with a significantly lower input energy of 140 MeV. As can be seen from Fig. 17, the cooling efficiency improves slightly with respect to the case of 200 MeV. The maximum value is still around 10%. The performance of a system with 8 cavities cannot be reached.

To summarize the cooling performance for a system of 4 cavities, we consider an input emittance of 5000 mm mrad, for which the transmission is 100%. For this input emittance and the two input energies considered, the cooling efficiency is summarized in Tab. 3. The solenoid field in the cooling cell has values of 2.7 T (200 MeV) and 2.5 T (140 MeV). For an input energy of 140 MeV the cooling performance is hence better and lower solenoid fields are required.

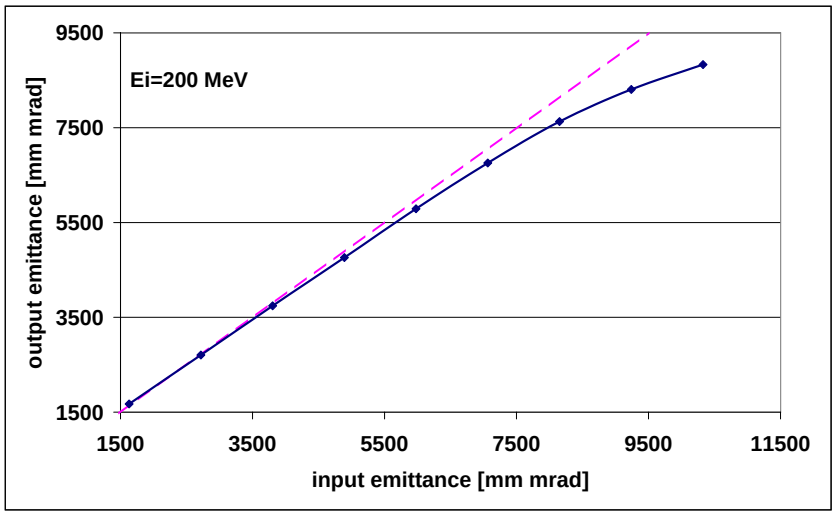

Figure 14: Output emittance versus input emittance (r.m.s., normalized) for a channel of 4 cavities and an input beam energy of 200 MeV. The dashed line represents $\varepsilon_{out} = \varepsilon_{in}$.

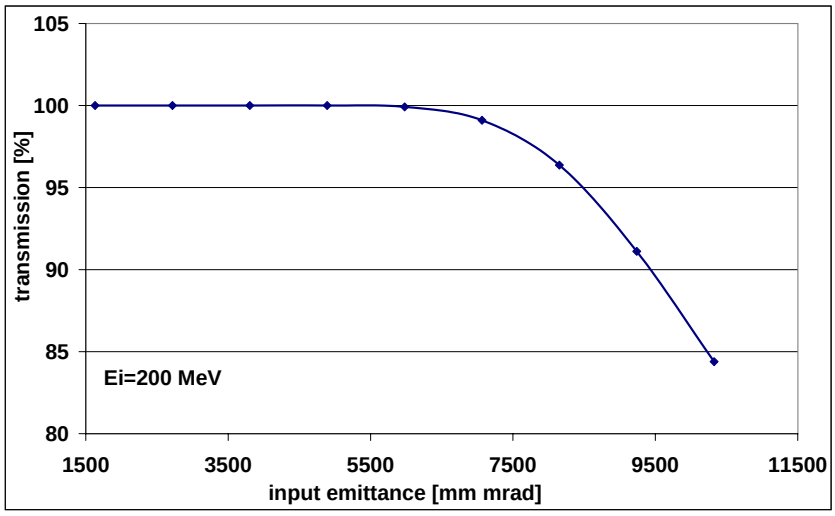

Figure 15: Transmission versus input emittance (r.m.s., normalized) for a channel of 4 cavities and an input beam energy of 200 MeV.

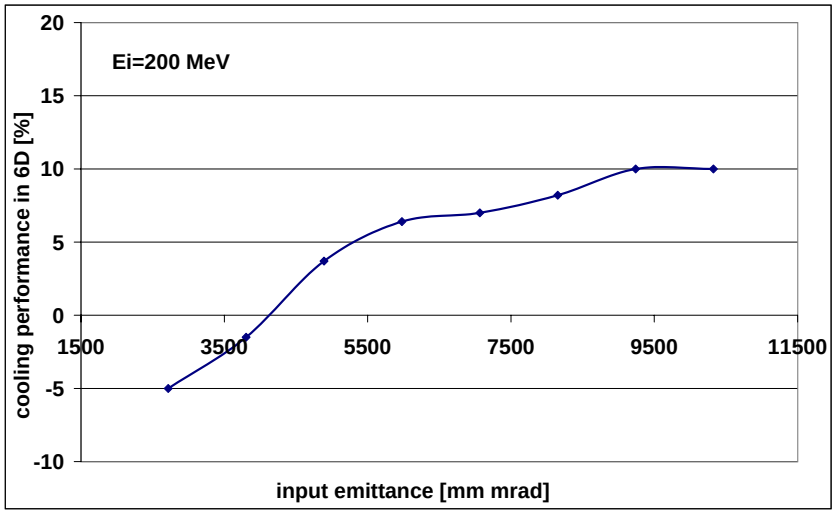

Figure 16: Cooling efficiency versus input emittance (r.m.s., normalized) for a channel of 4 cavities and an input beam energy of 200 MeV.

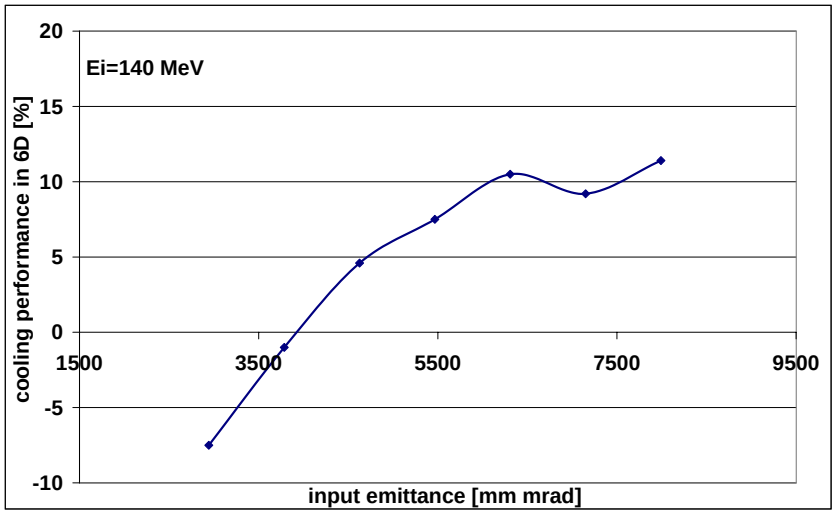

Figure 17: Cooling efficiency versus input emittance (r.m.s., normalized) for a system of 4 cavities and an input beam energy of 140 MeV. There is a slight improvement in cooling efficiency by going to lower beam energy but the performance of a system with 8 cavities cannot be reached. Note, that the results are subject to fluctuations (statistical processes in the absorbers) which can explain the bump around 7500 mm mrad.

E_{in} [MeV]	cooling efficiency [%]	solenoid field [T]
200	4.5	2.7
140	6.5	2.5

Table 3: Comparison of cooling efficiency for ε_{in}=5000 mm mrad (r.m.s., normalized) and two different input beam energies.

2.6 Cross Check of PATH and ICOOL Simulations

The results obtained from PATH have been reproduced using the code ICOOL. The same input beam distribution and the same channel optics were used. The simulations were done with a total of 50000 particles. Figure 18 shows the transverse emittance versus z as computed with ICOOL. Excellent agreement with the corresponding plot for PATH (Fig. 5) is found. The cooling performance for the example case studied is summarized in Tab. 4.

Figures 19 and 20 show the horizontal and vertical r.m.s. emittance (normalized) as computed by the two codes along the channel.

	PATH	ICOOL
transmission	100%	100%
transv. emittance reduction	3.7%	3.2%
particle gain in 6D volume	9.1%	7.6%

Table 4: Comparison of PATH and ICOOL results for one example case.

3 200 MHz Option

3.1 Layout

As a possible alternative to the scenario using 88 MHz cavities, we have studied a cooling experiment based on 200 MHz cavities. The goal of this study was to verify the possibility of using the cavities at 200 MHz with the same beam characteristics as in the 88 MHz case, and compare the cooling performances. If pill-box cavities resonating at 200 MHz with conductive irises are used, it is not possible to integrate the solenoids into the cavities as in the case of the 88 MHz cavities (Section 2.1) [6]. The set-up for this scheme is therefore different from that at 88 MHz.

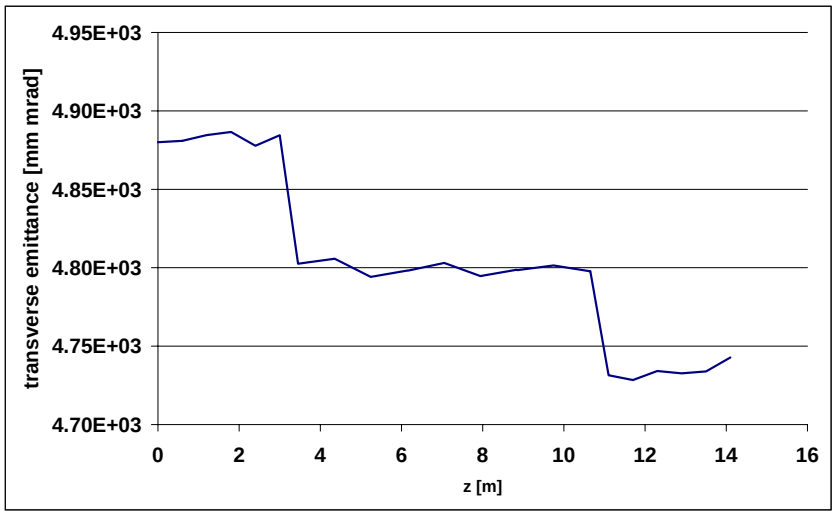

Figure 18: Transverse emittance (r.m.s., normalized) along the cooling channel as computed by ICOOL.

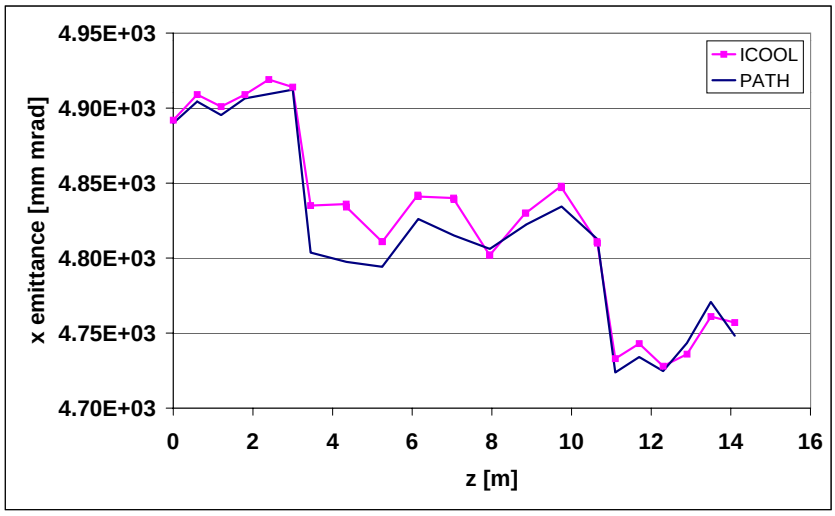

Figure 19: Horizontal emittance (r.m.s., normalized) along the channel of 8 cavities as computed by PATH and ICOOL.

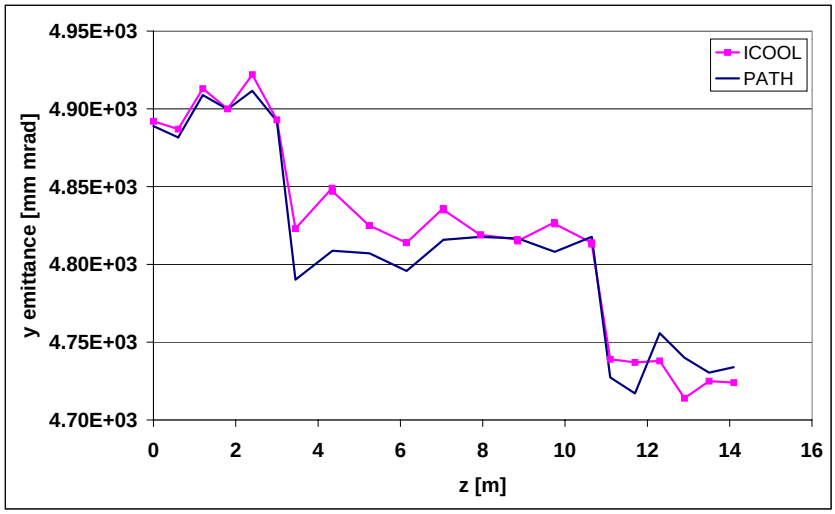

Figure 20: Vertical emittance (r.m.s., normalized) along the channel of 8 cavities as computed by PATH and ICOOL.

We have simulated a system based on the engineering constraints given in the US study II proposal [2]. In the US proposal there are two possible schemes: SFOFO lattice 1 and 2. Preliminary simulations [7] showed that the second scheme, with groups of two cells separated by solenoids, gives a more uniform magnetic field and better performances. We have therefore based our simulations on this set-up. However, it is important to point out that in our case the beam dynamics is different from the one reported in [2]. The design has been slightly modified, and the magnetic field is different. Furthermore, in our simulations we do not alternate the polarity of the solenoids. Although a scheme with equal solenoid polarity is not the one proposed for the full-scale cooling channel, it can give a demonstration of muon cooling and it is cheaper to generate the required magnetic field.

The solenoid configuration is illustrated in Figure 21 where the magnetic field lines as computed with the POISSON code [8] are shown. In the input and output diagnostic sections there are two continuous solenoids with a radius of 33 cm and length of 2 m. At the entry of the cooling channel there is a 47 cm long liquid hydrogen absorber inserted inside a solenoid of 21 cm inner radius. The absorber is followed by a system of two cavity cells resonating at 200 MHz with an average effective gradient of about 11.8 MV/m. In the middle of the cells and outside of them there is a short solenoid (18 cm) with a large radius of 61.5 cm. After the two cells there is another 40 cm long solenoid with an aperture of 21 cm that contributes to maintain the magnetic field as uniform as possible.

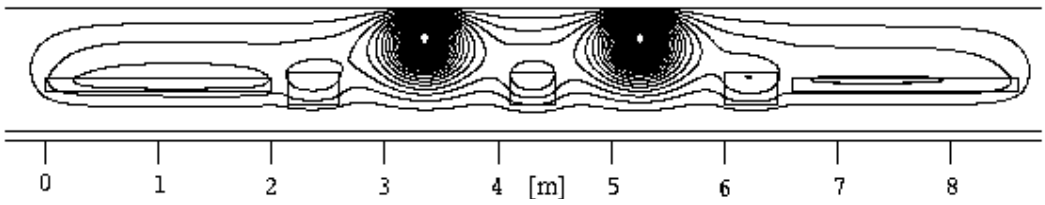

Figure 21: Magnetic field lines computed with POISSON.

The second part of the cooling channel is identical to the first one with two more cavity cells followed by the exit absorber. The total length, including diagnostics, is 8.6 m, and we have assumed a physical aperture of 20 cm. The total energy lost in the absorbers at a kinetic energy of 200 MeV corresponds to the energy gained in the cavity system.

3.2 Beam Dynamics

The coil arrangement shown in Fig. 21 results in a magnetic field as shown in Figs. 22 and 23. With this solenoid field we obtain the emittance diagram shown in Figure 24. [p] For a kinetic energy of 200 MeV and $\Delta E = \pm 30$ MeV, the final normalized rms emittance is 4630 π mm mrad, which, compared to the input emittance of 4900 π mm mrad, gives a reduction of about 5.6 % with a particle transmission of 100 %. The initial beam parameters are the same as used in the 88 MHz simulations, i. e. $\beta = 1$ m, $\alpha = 0$, and the number of particles is $N = 50000$. The cavity system is set to work on crest. If we define the cooling efficiency as the increase of the number of particles inside a given acceptance, and use as acceptance 15000 π mm mrad (normalized) in both transverse dimensions, we get an efficiency of 8.8 %.

Similarly to what has been done for the 88 MHz case, we show in Figure 25 the output versus input emittance. For an input emittance of about 3000 π mm mrad (r.m.s. normalized) the equilibrium emittance is reached. Below this threshold the beam is heated. The transmission remains 100 % up to the maximum emittance that we have simulated, 10000 π mm mrad, as the aperture used for this set-up is larger than that of the 88 MHz channel. In Figure 26 we show the cooling efficiency, as defined above, for a range of input r.m.s. emittance. It is negative for small input emittances (heating) and goes up to about 20 % for the largest input emittance.

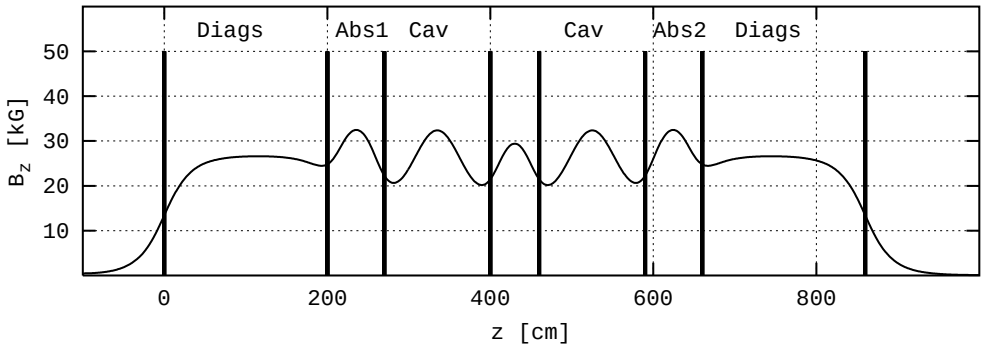

Figure 22: Longitudinal magnetic field on axis.

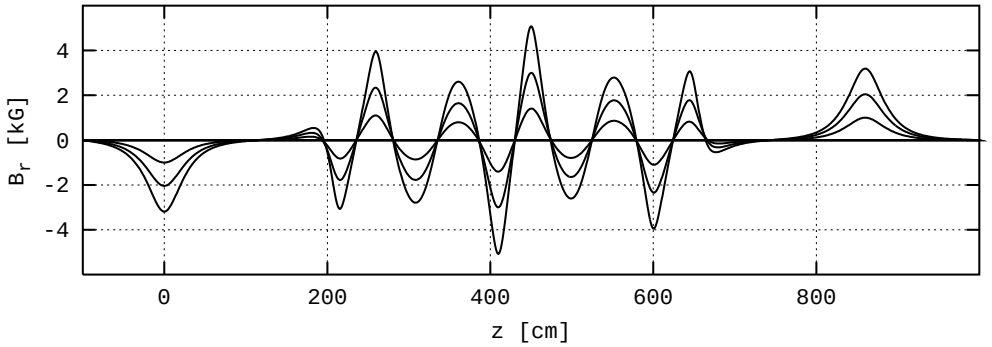

Figure 23: Radial magnetic field at r = 0, 5, 10, 15 cm.

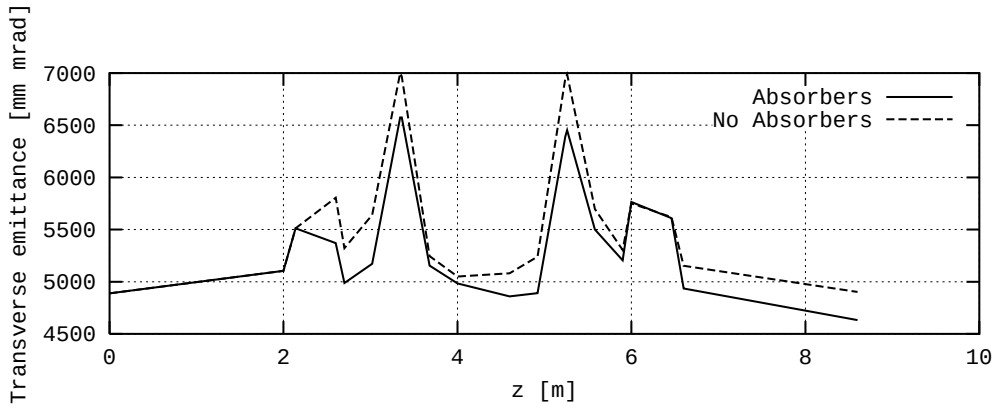

Figure 24: Transverse emittance (r.m.s., normalized) along the channel with and without absorbers.

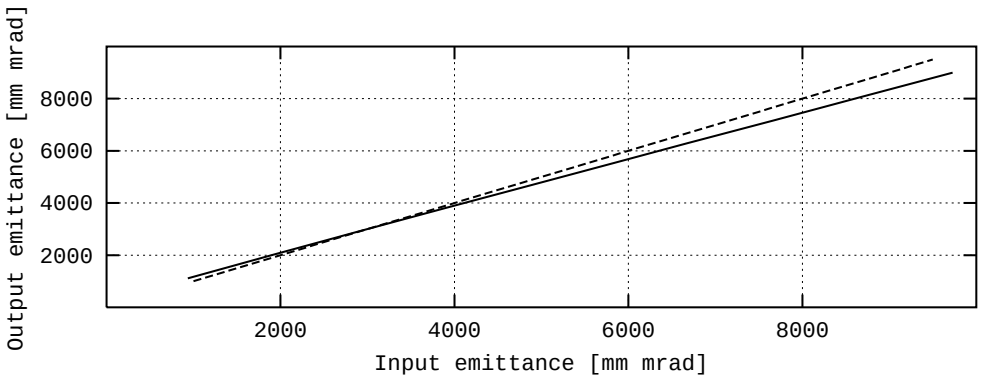

Figure 25: Output emittance vs input emittance (r.m.s., normalized) at 200 MeV (PATH simulation using 50000 particles).

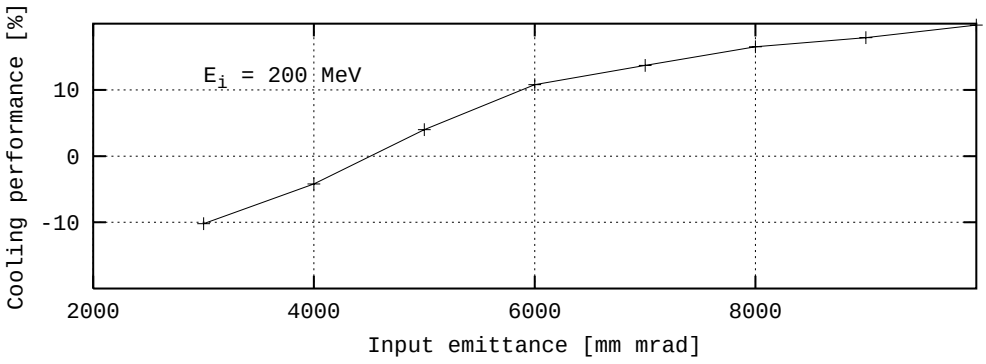

Figure 26: Cooling efficiency vs input emittance (r.m.s., normalized) for an input beam of 200 MeV (PATH simulation using 50000 particles).

3.2.1 Influence of Beam Energy

We have run the setup at different input beam energies, adjusting slightly the solenoid field. In Figures 27 and 28 we show the results for energies of 140 MeV and 230 MeV respectively. Also in these two cases the transmission is about 100 % up to the largest input emittance.

3.2.2 Magnetic Field Variation

With the scheme of the cooling channel that we have illustrated in the previous sections, it is possible to change the solenoid currents and work with other values of the magnetic field. For example, with the magnetic field shown in Figure 29 (on axis), which is about a

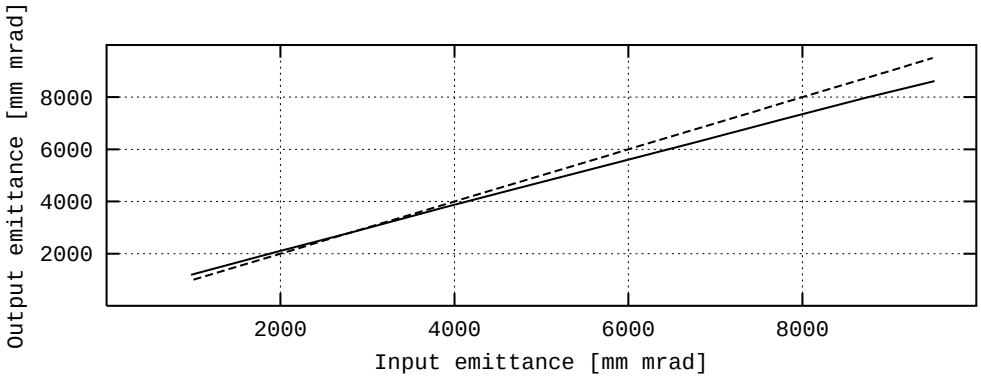

Figure 27: Output emittance vs input emittance (r.m.s., normalized) at 140 MeV (PATH simulation using 50000 particles).

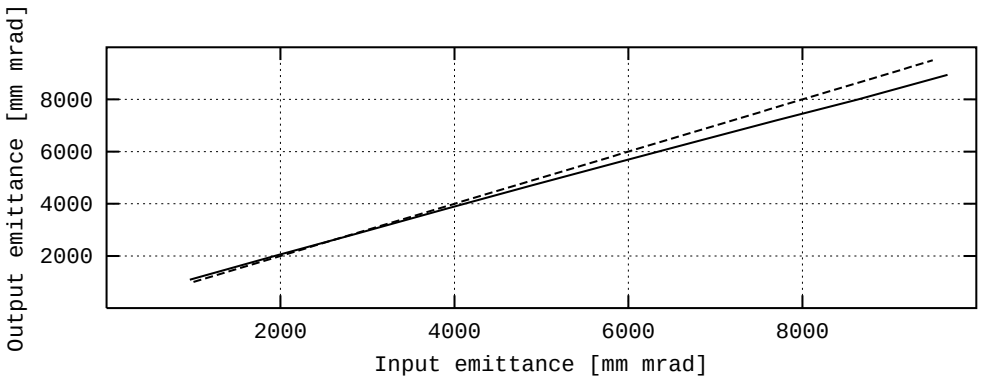

Figure 28: Output emittance vs input emittance (r.m.s., normalized) at 230 MeV (PATH simulation using 50000 particles).

factor of 1.5 higher than in the reference case, the same cooling performance is achieved even if the emittance along the channel (Fig. 30), is higher than that of Figure 24. This demonstrates the flexibility of the proposed scheme.

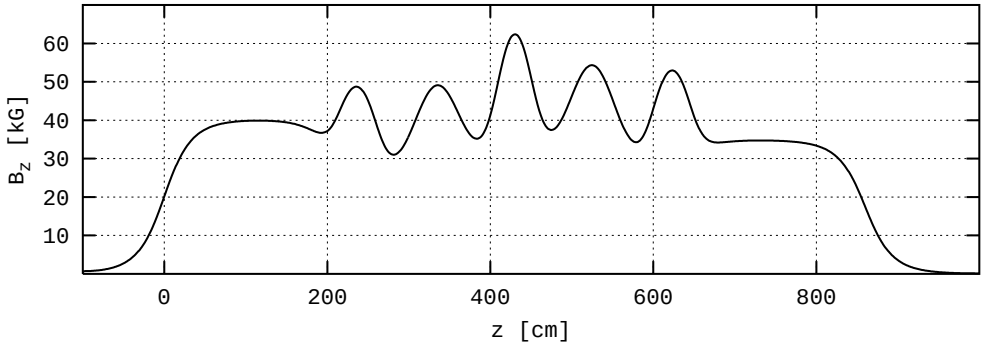

Figure 29: Alternative longitudinal magnetic field.

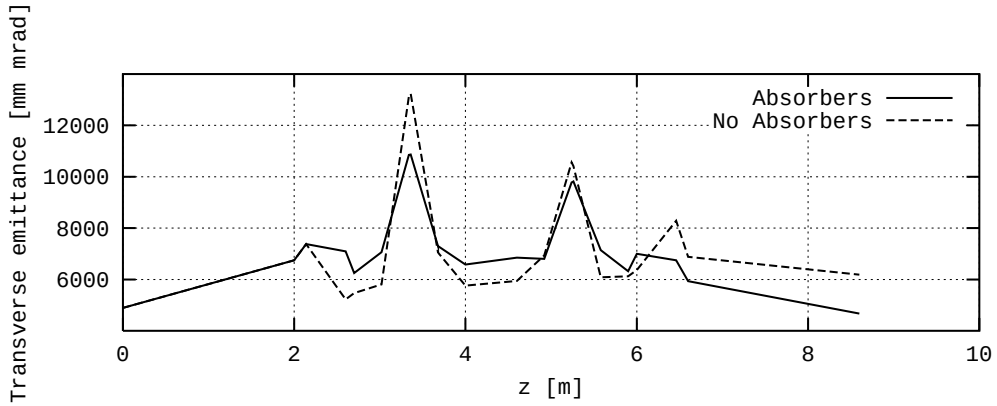

Figure 30: Transverse emittance (r.m.s., normalized) along the channel with and without absorbers for the magnetic field of Figure 29.

4 Figure of Merit for the Cooling Experiment

In the cooling channel of the Neutrino Factory the relevant figure of merit is the increase of the number of muons in the acceptance of the downstream accelerators. This acceptance is defined independently in the three planes (x, y and longitudinal). To increase the figure of merit, correlations between the planes have to be minimized at the point of transition from solenoidal focusing to quadrupole focusing.

In the cooling experiment, the emittances are measured inside the solenoid field. If the beam dynamics of the experiment is not chosen to minimise inter-plane correlations, there is no possibility to compensate for these correlations. In a general solenoidal beam transport correlations will mainly develop between the x and the y plane. Therefore, an algorithm was developed to count particles in 4D or 6D hyper-ellipsoids, to be used as figure of merit for the cooling experiment in the presence of inter-plane correlations [9]. It allows to measure 4D and 6D cooling rather than the 2D projections.

Figure 31 shows the number of muons inside a normalized 4D volume of ($15000\ \pi$ mm mrad)^2 as a function of distance for the 88 MHz cooling experiment (simulated in ICOOL). The upper curve is the number of muons in a 4D ellipsoid and the lower one in the 2D projections. In this experimental setup the correlations between the x and y plane stay below 0.08 along the channel. Therefore, there is no great difference between the two curves. The 4D ellipsoid looks at a more central core of the distribution, yielding a higher density of muons and a slightly larger figure of merit (9.9% increase as compared to 7.6% in the 2D projections). Figure 32 shows the corresponding plot for the 200 MHz

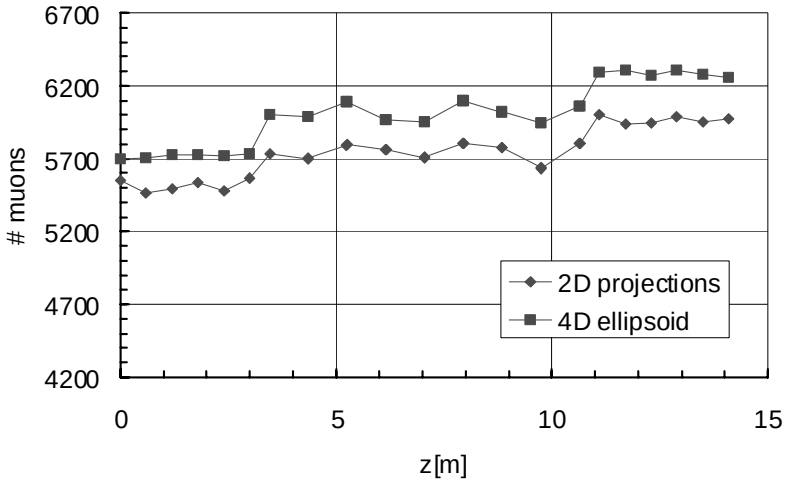

Figure 31: Number of muons inside 4D volume of (1.5 π cm rad)^2 for a cooling experiment at 88 MHz (8 cavities).

cooling experiment (PATH simulation). Values are shown at the beginning and the end of the experiment and at two points in the middle, where $\epsilon_x \times \epsilon_y$ peaks (at 3.4 m and 5.2 m, compare to Figure 24). The inter-plane correlations are 0, 0.7, 0.6 and 0.14 respectively at the 4 analysed positions. At the points of high correlation, the method of 2D projections does not give a useful result for measuring the cooling performance of the experiment.

The figure of merit calculated in the 4D ellipsoid and the 2D projections is 13.3% and 9.9% respectively. Counting the muons in 4D or 6D yields a stable figure of merit in the

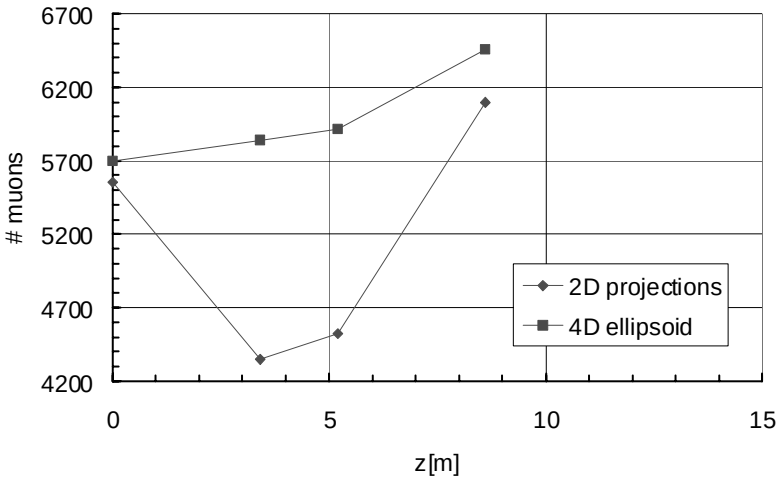

Figure 32: Number of muons inside a 4D volume of (15000 π mm mrad)^2 for a cooling experiment at 200 MHz.

presence of correlations. The 4D ellipsoid looks at a more central core of the distribution and has therefore a higher density of muons and a slightly higher figure of merit than in the 2D projections.

The two simulations use the same particle input distribution of 10^4 muons. The energy loss and gain, in absorbers and cavities respectively, is 4.4% higher in the 200 MHz experiment. The muon energy is 200 MeV $\pm$ 30 MeV in both cases. The average magnetic field at the absorber is 1.95 T in the 88 MHz setup and 3.04 T in the 200 MHz case. This methode gives a comparable figure of merit for the two experiments.

5 Conclusion

We have simulated two possible scenarios for a muon ionization cooling experiment at 88 and 200 MHz with the goal of comparing them from a beam dynamics point of view. In particular, we were interested in the cooling efficiency, which has to be well in the range of the proposed emittance diagnostics [10]. We find that in terms of cooling efficiency both schemes show a comparable performance. The set-up at 200 MHz has a naturally higher acceleration gradient than the one at 88 MHz, which results in a better cooling rate per meter. However, the overall cooling performance of the two systems (8 cavities

at 88 MHz versus 4 cavities at 200 MHz) is, as the total absorber length is the same, comparable. The choice of frequency is therefore a technical one, i.e. for a required minimum cooling efficiency one has to consider the total length of the system, number of cavities used, achievable gradient and rf power.

A major difference between the two schemes is the arrangement of the solenoids. The large bore solenoids between and around the 200 MHz cavities result in a magnetic field pattern which is less homogeneous than in the case of the 88 MHz cavities, where the solenoids are integrated in the cavity such that they are close to the beam and periodic. Consequently, for the set-up at 88 MHz, the emittance evolution is very smooth and there is little coupling between the planes. For the 200 MHz system, the coil arrangement and hence the magnetic field along the channel vary much more. This results in strong coupling.

As can be seen e.g. in Fig. 5, in case of the 88 MHz set-up the emittance evolution along the channel is very smooth and flat in the solenoids, while it drops down in the absorbers. In the case of the 200 MHz set-up, the transverse emittance performs oscillations which are due to coupling between the planes.

Another technical difference is the one that the 200 MHz cavities have to be separated by conducting windows in order to achieve the required gradient. This could result in unacceptable high dark current. Also, windows might break during cavity conditioning. In the 88 MHz cavities no windows are required.

6 Acknowledgements

This paper includes important contributions by Arnaud Perrin who passed away in a tragic accident.

References

[1] A. Lombardi, *A 40-80 MHz System for Phase Rotation and Cooling*, CERN Neutrino Factory Note 37 (2000).

[2] S. Ozaki, R. Palmer, M. Zisman, J. Gallardo (ed.), *Feasibility Study-II of a Muon-Based Neutrino Source*, BNL-52623 (2001).

[3] R. Garoby, F. Gerigk, *Cavity Design for the CERN Muon Cooling Channel*, CERN Neutrino Factory Note 87 (2001).

[4] S. Russenschuck, M. Aleksa, private communication.

[5] K. Hanke, E. S. Kim, *Beam Dynamics Study of a Cooling Experiment based on the 88 MHz CERN Cooling Channel,* CERN Neutrino Factory Note 90 (2001).

[6] F. Tazzioli, private communication.

[7] M. Migliorati et al., *Preliminary Study of the Cooling Channel based on the 200 MHz Cavities*, presented at the Workshop on a Muon Ionization Cooling Experiment, October 25-27, 2001, CERN.

[8] J. H. Billen, L. M. Young, *Poisson Superfish*, Los Alamos National Lab report LA-UR-1834.

[9] E. B. Holzer, CERN Neutrino Factory Note 111, in preparation.

[10] P. Janot, private communication.